ACS OMEGA

Open Access

http://pubs.acs.org/journal/acsodf

Article

Screening of Metal Oxides and Hydroxides for Arsenic Removal from Water Using Molecular Dynamics Simulations

Noor E. Hira, Serene Sow Mun Lock,* Ushtar Arshad, Khadija Asif, Farman Ullah, Abid Salam Farooqi, Chung Loong Yiin, Bridgid Lai Fui Chin, and Zill e Huma

Cite This: *ACS Omega* 2023, 8, 48130−48144

Read Online

ACCESS | Metrics & More | Article Recommendations

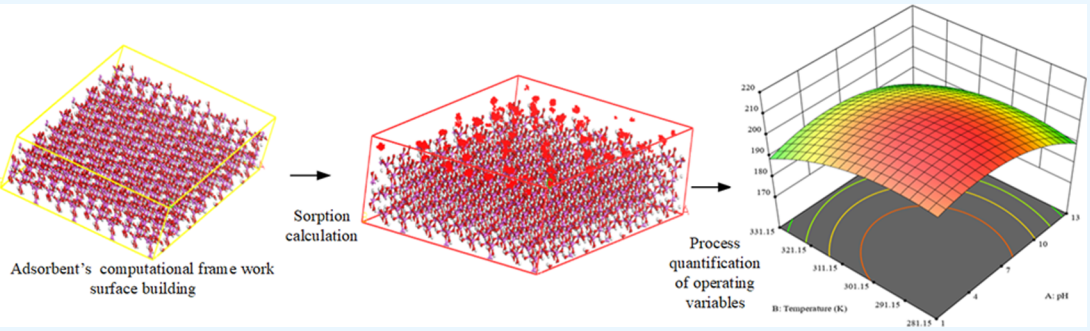

ABSTRACT: Arsenic in groundwater is a harmful and hazardous substance that must be removed to protect human health and safety. Adsorption, particularly using metal oxides, is a cost-effective way to treat contaminated water. These metal oxides must be selected systematically to identify the best material and optimal operating conditions for the removal of arsenic from water. Experimental research has been the primary emphasis of prior work, which is time-consuming and costly. The previous simulation studies have been limited to specific adsorbents such as iron oxides. It is necessary to study other metal oxides to determine which ones are the most effective at removing arsenic from water. In this work, a molecular simulation computational framework using molecular dynamics and Monte Carlo simulations was developed to investigate the adsorption of arsenic using various potential metal oxides. The molecular structures have been optimized and proceeded with sorption calculations to observe the adsorption capabilities of metal oxides. In this study, 15 selected metal oxides were screened at a pressure of 100 kPa and a temperature of 298 K for As(V) in the form of $HAsO_4$ at pH 7. Based on adsorption capacity calculations for selected metal oxides/hydroxides, aluminum hydroxide ($Al(OH)_3$), ferric hydroxide (FeOOH), lanthanum hydroxide $La(OH)_3$, and stannic oxide (SnO_2) were the most effective adsorbents with adsorption capacities of 197, 73.6, 151, and 42.7 mg/g, respectively, suggesting that metal hydroxides are more effective in treating arsenic-contaminated water than metal oxides. The computational results were comparable with previously published literature with a percentage error of 1%. Additionally, SnO_2, which is rather unconventional to be used in this application, demonstrates potential for arsenic removal and could be further explored. The effects of pH from 1 to 13, temperature from 281.15 to 331.15 K, and pressure from 100 to 350 kPa were studied. Results revealed that adsorption capacity decreased for the high-temperature applications while experiencing an increase in pressure-promoted adsorption. Furthermore, response surface methodology (RSM) has been employed to develop a regression model to describe the effect of operating variables on the adsorption capacity of screened adsorbents for arsenic removal. The RSM models utilizing CCD (central composite design) were developed for $Al(OH)_3$, $La(OH)_3$, and FeOOH, having R^2 values 0.92, 0.67, and 0.95, respectively, suggesting that the models developed were correct.

1. INTRODUCTION

Water contamination is a critical challenge at a global level. Drinking toxic water impacts millions of people worldwide, and our ecosystem has suffered consequently.[1] As population and industrialization rise, access to potable water becomes increasingly challenging.[2−4] Arsenic levels in many countries like Pakistan, Bangladesh, China, Taiwan, America, India, and Mexico are alarmingly high.[5−9] It has been classified as carcinogenic and poisonous.[10,11] It can cause liver, kidney,

Received: September 14, 2023
Revised: November 9, 2023
Accepted: November 24, 2023
Published: December 8, 2023

lung, and bladder cancer if ingested continuously, even in minute amounts (ppb).[12−14] The WHO (World Health Organization) current maximum allowable arsenic concentration in drinking water is 10 g/L (ppb).[15−17] Nonetheless, many developing nations continue to adhere to the previous guideline of 50 g/L due to inadequate infrastructure and costly water treatment technologies.[13] In July 2018, China hosted the seventh International Congress on Arsenic in the Environment, which included sustainable management and mitigation of arsenic removal.[18] The United Nations (UN) members stated an agreement on the 2030 Agenda for Sustainable Development, which aimed to guide national and international initiatives in the next 15 years, highlighting the importance of paying attention to arsenic removal so everyone has access to clean water.[18]

Several arsenic removal methods have been utilized, including coagulation, adsorption, ion exchange, and membrane separation.[15,19] Adsorption is thought to be the most appropriate and effective approach for removing toxins from water and wastewater due to its high effectiveness and low cost.[20,21] In this context, adsorption processes do not contribute to unwanted byproducts and have been found to be superior to other wastewater treatment methods in terms of ease of design and operation. Adsorbents of several kinds, such as zeolites, oxides, hydroxides, carbon-based materials, metal−organic frameworks, and clay, have been developed for the adsorption process.[20] Each adsorbent tends to remove pollutants from water and wastewater and has potential advantages. Adsorption is a surface phenomenon, and these adsorbents sorb the pollutants on their surface to remove them from water and wastewater.[22,23] The adsorption phenomenon arises from disparate or persistent attractive forces acting on the surface particles of the adsorbent material. Unlike the particles within the bulk adsorbent, these forces are not uniformly balanced. Consequently, the particles located at the surface of the adsorbent exhibit a notably elevated energy state compared to those situated within the core. Surface energy is this additional energy per unit surface area, and it is necessary for the attraction of adsorbate to its adsorbent surface.[24] The enthalpy and entropy are other important factors to be taken into account for adsorption.[25] Enthalpy and entropy are the measures of a potential sorption process.[25] The pollutants on adsorbents' surfaces are adsorbed, consequently being removed from contaminated water.[23]

Adsorption is one of the finest ways to remove arsenic from water with reported >95% quantitative efficiencies for arsenite and arsenate remediation. It is effective and affordable, does not require chemical addition, and is simple to use in developing countries with insufficient skilled labor and unstable electricity supplies.[26] These advantages of adsorption have encouraged many researchers to employ it to remove arsenic from drinking water.[12,27] In addition, adsorption is considered more adaptable than ion exchange, easier to run and safer to handle than the contaminated sludge produced by coagulation/precipitation, and cheaper than membrane separation.[28] Metal oxides/hydroxides, zeolites, and other adsorbents are commonly used in adsorption.[20] Among these adsorbents, metal oxides and hydroxides can eliminate arsenic more effectively, since surface functional groups, typical oxygen-containing groups, assist in its removal.[29] Arsenic removal involves chemisorption, forming inner-sphere complexes during the removal process in which As(V) directly binds to oxygen.[4]

Many experimental studies for arsenic removal from water have been reported by using different adsorbents. Initially, iron and $Al(OH)_3$ were investigated experimentally for arsenic removal from water.[30] Later, iron oxide ($F_{e2}O_3$) and aluminum oxide (Al_2O_3) were examined by experimental work, and it was found that they were effective by having maximum As(V) uptake values of 0.66 mg/g Fe_2O_3 and 0.17 mg/g Al_2O_3 at pH 6.[27] In a later study, the ultrafine Fe_2O_3 nanoparticles were experimentally checked for As(III) and As(V) adsorption, and it was found that Fe_2O_3 nanoparticles have adsorption capacities of 95 and 47 mg/g, respectively.[31] In another study, arsenic removal from water using FeOOH and Fe_3O_4 was studied, and it was observed that arsenic removal from water using iron oxides was pH dependent, and the maximum arsenic removal percentage was 80%.[32] Later, synthesized FeOOH was also studied for the adsorption of arsenic, in which the experimental equilibrium data were well represented by the Langmuir isotherm, and an estimated adsorption capacity of 76 mg/g was reported at ambient temperature, which was significantly higher than most of the adsorbents reported in the previous literature.[33] In a review, it was reported that for arsenic removal from water by adsorption using iron oxide, FeOOH was declared as a good adsorbent by having different adsorption capacities from 5 to 443 mg/g, which were highly dependent upon operating conditions, such as pH and temperature.[28] The removal of arsenic from water using iron-based adsorbents was reviewed, and it was concluded that iron oxides and hydroxides were effective adsorbents for arsenic removal.[34] In recent experimental studies, it was found that the arsenic adsorption rate is related to pH values. Arsenic adsorption was favored under acidic pH values and rapidly decreased in basic media.[35] In another recent work, Yoon et al. studied As(V) removal utilizing lignin and iron chloride to create biochar with low basicity and found highest As(V) adsorption, with a removal efficiency of >77.6% at the pH range of 3.0−10.[12] It was also mentioned that both the adsorbent and the adsorbate were involved in the adsorption process; this shows that As(V) was adsorbed by magnetite by a specific chemical reaction (chemisorption). As(V) binding to magnetite has been described as occurring mostly through chemisorption, which involves the development of bidentate inner-sphere complexes.[12] Xion et al. studied schwertmannites and akaganéites for the adsorption of arsenic ions from contaminated water and found that the adsorption of As(III) and As(V) was a rapid reaction, in line with the pseudo-second-order rate equation. It was also mentioned that iron oxyhydroxides exhibited exceptional adsorption capacities to arsenic species due to their abundant hydratable hydroxyl groups, which can form inner-sphere complexes with arsenic on their surface.[36]

Apart from performing experimental work for arsenic removal, many simulation studies have been done using molecular dynamics (MD) simulations.[37] The MD simulation allows for the microscopical study of the adsorption process within a sufficient time frame, budget, and space. Molecular modeling is currently regarded as a successful research method for elucidating the adsorption process.[20,38] MD simulations can produce effective techniques to simulate structures and elucidate the adsorption phenomenon at a molecular level by applying appropriate computational computations.[39,40] Moreover, recently, molecular simulations have evolved as a prominent technology for the screening of materials in industrial applications. It has been performed to circumvent

https://doi.org/10.1021/acsomega.3c07014
ACS Omega 2023, 8, 48130−48144

the limitations of experimental apparatus and materials.[41] In addition, it offers a platform for studying the molecular-level interpretation of quantities such as energy, enthalpy, and sorption distribution, which surpasses the capability of experimental scale measurement.[42−44] Therefore, computational works are emerging because experimental work can be very expensive, time-consuming, and often difficult to handle under extreme conditions, i.e., high pressure and temperature.

Previously, a molecular simulation study was performed to understand the arsenate reaction kinetics with FeOOH, which revealed that the physical adsorption process proceeded with Gibbs free energies of the reaction between −21 and −58 kJ/mol.[42] The highest Gibbs free energy of the reaction for physical adsorption was produced by the hydrogen bonding between H atoms on FeOOH and O atoms in arsenate.[42] In a simulation study to understand the mechanism and stability of the As(V)−Fe(III) oxyhydroxide coprecipitate over a broad pH range, it was found that the adsorption energies for monomeric, dimeric, and trimeric complexes were −61.35(1−1), −65.50(2−1), and −71.8(3−1) kcalmol^{-1}, respectively, which indicated that the formed complexes were very stable.[45] Later, the phenomenon was studied by using a Monte Carlo simulation approach for the adsorption of toxic ions on iron oxide nanocrystals. The amount of removed As(V) ions might range between 10 and 90%, depending on the choice of the nanocrystal morphology, suggesting that the adsorbent surface and structure played an important role.[7] In a recent simulation study for arsenic removal from water, it was found that the orientation of the adsorbate molecule and its distance from the adsorbent affected the adsorption phenomenon.[46] In another work for arsenic removal from water, the binding energy (E_b) was calculated using density functional theory (DFT) simulations, and it was found that the adsorption amount depends on the binding energy value. The more the binding energy value of arsenic species with the adsorbent, the more the adsorption amount.[47]

From a review of the literature, it was found that the simulation research work for arsenic removal from water using adsorption was restricted as compared to the number of experimental results available. Most computational works were confined to study the removal of arsenic using iron oxides among the oxide and hydroxide families. Moreover, it was found that simulation studies were mostly focused on understanding the phenomenon at the atomistic level limited to few adsorbents, typically on observing the interaction of arsenic with the material and studying structural bonding and stability rather than elucidating the macroscopic behavior via computation of adsorption capacity.[42,45] On the other hand, experimental studies focused mostly on determining adsorption capacity for specific metal oxides and hydroxides only at different and limited experimental conditions in the quest for the optimal performance for arsenic removal from water.[27,31] This research work is a pioneering study to elucidate sorption phenomena and simultaneously calculate adsorption capacity for each adsorbent to achieve finer screening of adsorbents for arsenic removal from water. Moreover, it unravels the effect of three parameters under a wide range of operating conditions, e.g., pH, temperature, and pressure, to elucidate how each influences the loading capacity of that heavy metal. To the author's best knowledge, previously, sorption loading was not employed to calculate adsorption capacity in the screening of adsorbents for arsenic removal in wastewater treatment.[38]

For this study, 15 metal oxides/hydroxides, which were commonly applied in water treatment, were investigated. Selected metal oxide/hydroxide structures were constructed and validated using Material Studio (MS) software.[20,39,43] The sorption loading was determined using the Sorption module that enabled adsorption capacity to be determined for the screening of the adsorbents. After the screening process, selected adsorbents were proceeded with operating variable study, regression modeling, and optimization using Design-Expert (DOE) software.[48,49] The adsorption behavior was studied at different pH ranges (1−2, 3 to 7, 7−11, and 11 onward), a wide range of temperatures in Kelvin (K; 281.15, 291.15, 301.15, 311.15, 321.15, and 331.15 K), and a broad domain of pressures in kilopascal (kPa; 100, 150, 200, 250, 300, and 350 kPa). An appropriate regression model was developed to describe the effect of operating variables on the adsorption capacity for screened adsorbents ($Al(OH)_3$, $La(OH)_3$, and FeOOH) using center composite design (CCD).

2. METHODOLOGY

The software used to carry out the molecular simulation investigation in the present work was BIOVIA Materials Studio (MS) version 8.0.[20] It was used to carry out an atomistic simulation where interactions were represented by empirical potential functions to integrate the standard equations of motion as positions of each atom were recorded.[20,41]

The molecular simulation methodology of this study is described in two sections. The specifications of the MD simulation are listed in Table 1. The framework and simulation

Table 1. Operational Modules and Specifications for This Molecular Simulation Work

module	specification	references
forcite	task: geometry optimization	39,61−64
	algorithm: smart	
	quality: medium	
	force field: universal	
	summation method: *E*wald	
	max. iterations: 500	
forcite	task: dynamics	41,43,64−66
	quality: medium	
	force field: universal	
	electrostatics: atom based	
	dynamics ensemble: NVT	
	temperature: 298 K	
build tool	cleave plane (*hkl*): (−1 0 0)	67−69
	supercell: 4 × 4	
	vacuum slab thickness: 5.0 A	
sorption	task: fixed pressure	20,64,70
	method: metropolis	
	quality: medium	
	force field: universal	
	fugacity: 100 kPa	
	temperature: 298 K	

basis for structure construction, geometry optimization, validation, and surface building are addressed in Section 2.1, while Section 2.2 outlines the sorption loading, and adsorption capacity calculations and empirical modeling are included in Section 2.3. The adsorption capacities of 15 materials were determined using MS software employing Monte Carlo

https://doi.org/10.1021/acsomega.3c07014
ACS Omega 2023, 8, 48130−48144

simulations.[20,50] Ferric oxyhydroxide (goethite, FeOOH), ferric oxide (hematite, Fe_2O_3), ferrous ferric oxide (magnetite, Fe_3O_4), aluminum oxide (Al_2O_3), titanium dioxide (TiO_2), aluminum hydroxide $Al(OH)_3$, zirconium oxide (ZrO_2), silver oxide (Ag_2O), lanthanum oxide (La_2O_3), stannic oxide (SnO_2), lanthanum hydroxide ($La(OH)_3$), tin oxide (SnO), zinc oxide (ZnO), ferrous oxide (FeO), and silicon oxide (SiO_2) were chosen for arsenic adsorption based on their application in the field of water treatment.[7,10,20,27,28,51−60]

2.1. Structure Construction and Geometry Optimization. In this section, the computational frameworks that were used for the simulation of adsorbents in this work are discussed in detail. The structures were imported from MS and Crystallographic Data Centre (CDC).[71] Using the Forcite module with a Universal force field, algorithm Smart, medium quality with summation method electrostatic Ewald, and atom-based van der Waals, the geometries of each of the metal oxide structures were optimized.[72] It was done by changing the bond distance and angles of the molecules.[65] The geometry was optimized to ensure structural stability via energy minimization.[62] The Universal force field was selected for whole molecular simulation calculations, since it could accurately anticipate the geometry and energy differences of organic molecules, inorganic molecules, and metal complexes.[38,64]

After geometry optimization, density calculations for structure validation were performed, which was done by selecting the Dynamics task in the Forcite module.[41] A canonical ensemble NVT (constant atom count, volume, and temperature) condition was employed, having a total simulation time of 5000 ps, with a time step of 1 fs, a *Q*-ratio of 0.01, and an energy deviation of 50,000.0 kcal/mol as integration tolerance criteria.[41,43] A Nose−Hoover−Langevin (NHL) thermostat was used for controlling the temperature at 298 K.[43,73] The summation methods used to calculate the electrostatic interactions and van der Waals interactions were the Ewald method with an accuracy of 0.001 kcal/mol and a buffer width of 0.5 Å and atom-based selections with a cutoff distance of 12.5 Å and truncation cubic spline having a spline width of 1 Å and a buffer width of 0.5 Å, respectively.[43,74] The density value obtained after NVT simulations was compared with the literature value for validation purposes.

Subsequently, an optimized surface structure was built by using the "Build" tool of the software. It included cleaving the surface, creating surface symmetry, and building the final structure by adding a vacuum slab.[75] All of the adsorbents' surfaces were cleaved on a (1 1 1) plane that had been used in previous simulation studies.[68,75,76] A larger surface was built using a supercell of order 4 × 4 using a symmetry tool and finally converted to a 3D lattice using the build vacuum slab function with a vacuum thickness of 5 A along the *c* direction.[63] The vacuum slab was added to avoid any impacts of adsorbed molecules with the periodic image of the adsorbent.[77]

2.2. Sorption Calculations. Sorption calculations were performed using the Sorption module of MS. For the screening of suitable adsorbents in arsenic removal, the Metropolis method was employed using the Universal force field at a constant temperature of 298 K and a fixed pressure of 100 kPa.[78] The selections were based on the practical observation that the majority of water treatment processes were performed at these ambient operating conditions, and previous simulation studies for water treatment were performed at 298 K.[63,79−84] The Metropolis method is a standard Monte Carlo simulation technique that treats the sorbent as a rigid structure and only accounts for sorbate translations and reorientations.[82] The fixed pressure sorption function, commonly known as grand canonical Monte Carlo (GCMC) simulations, was utilized to forecast the amount of the sorbate at the specified temperature and pressure using the Metropolis technique.[82] In this context, sorption at constant pressure and temperature replicated experimental circumstances and yielded the average sorbate component loading under the specified operating conditions. The arsenic sorption loading value within the metal oxide revealed its adsorption capability using the formula given in eq 1.

$$Q = \left[M \times \frac{L}{N_A}\right] \times \left[\frac{1}{V} \times \rho\right] \quad (1)$$

Here, Q = adsorption capacity, M = arsenic species molar mass, L = average loading, N_A = Avogadro's number, V = volume of the adsorbent, and ρ = density of the adsorbent.

It has been reported that arsenic exists in different ionic forms in water at different pH ranges. As(V) ions are the most prevalent forms of arsenic found in water and pose serious health risks to people, they are of tremendous interest from a research perspective.[85] As(V) mostly occurs as oxyanions of arsenic acid such as H_3AsO_4, $H_2AsO_4^{-1}$, $HAsO_4^{-2}$, and AsO_4.[30,86] It exists in the form of H_3AsO_4, $H_2AsO_4^{-1}$, $HAsO_4^{-2}$, and AsO_4^{-3} at pH 1, 3, 7, and 11, respectively.[86] The simulation was first performed for $H_2AsO_4^{-1}$ to represent treatment at pH 3 to be compared with results from the previous literature for FeOOH to validate the developed computational framework.[33] Subsequently, the research work was carried out for As(V) at pH 7 (in the form of $HAsO_4^{-1}$) to screen all of the selected metal oxides, and after screening, the operating variable effect was studied for the screened adsorbents.

After the suitable adsorbents for arsenic removal were evaluated, they were subjected to investigation at different operating conditions, including pH, temperature, and pressure. The temperature range was selected to be from 8 to 58 °C (281.15, 219.15, 301.15, 311.15, 321.15, and 331.15 K) due to different room temperatures at which drinking water treatment plants were operated attributed to seasonal variations.[87−89] With respect to operating pressure, most adsorption studies for water treatment were conducted at a pressure of 100 kPa while being mentioned in a report that feedwater pressure can vary from 100 to 277 kPa.[90] Hence, the selected range for pressure was 100−350 kPa.

2.3. Empirical Modeling. Design-Expert (DoE) software is frequently used to quantify the effect of process variables.[91] The process quantification for the effect of operating variables for arsenic removal was conducted based on the simulation runs generated by Design-Expert software (version 13) in the present study. The three chosen factors were quantified using response surface methodology (RSM) and central composite design (CCD) to achieve the goal of determining the optimal operating condition for arsenic removal from water.[91,92] CCD was selected because of its adaptability, dependability, and unceasing operation.[48] The current study used three operating conditions (factors), namely, pH (A), temperature (B), and pressure (C), for the response of adsorption capacity (mg/g) on FeOOH, $Al(OH)_3$, and $La(OH)_3$. The parameters were tested at different levels for combinations of different factors.

https://doi.org/10.1021/acsomega.3c07014
ACS Omega 2023, 8, 48130−48144

The lower and higher limits for the independent variable range are reported in Table 2.

Table 2. Factors and Levels are for Full-Factorial Design

factor	units	low level	high level
A: pH	H+ /OH− conc.	1	13
B: temperature	Kelvin	281.15	331.15
C: pressure	kPa	100	350

The interaction between the operational parameters, i.e., pH, temperature, and pressure, and response was studied using analysis of variance (ANOVA).[93] The *F*- and *p*-values were used to evaluate the fitted model for each relevant response in terms of the statistical significance of the operational parameters and interactions.

3. RESULTS AND DISCUSSION

3.1. Structure Validation and Geometry Optimization. First, geometry optimization was done using the Forcite module and the Universal force field, since the structure needed to be stable before performing the sorption task. The energy of all adsorbent structures was minimized, as shown in Figure 1, which depicts the optimization energy graph for FeOOH and $Al(OH)_3$. It was indicated that the initial enthalpies (energies) of the structures were 579.16 and 6718.25 kcal/mol, which were reduced to 341.18 and 4126.96 kcal/mol after geometry optimization, as illustrated in Figure 1a,b, respectively. The same procedure was done for all selected adsorbent structures for energy minimization.

Before building a structure, it was first validated by comparing the simulated density value for the adsorbent structure that was treated with NVT molecular dynamics using the Forcite module with literature-reported values. For all adsorbent structures, the simulated densities were in good agreement with experimentally reported observations with a percentage error of less than 8%. The results are reported in Table 3, and the structure after importing and building are given in Figure 2a,b, respectively.

3.2. Sorption Calculations. Sorption calculations were performed for all of the chosen metal oxides and hydroxides.

Table 3. Density Value Results are for Structure Validation

sr. no.	metal oxide	literature density (g/cm^3)	simulation density (g/cm^3)	percentage error (%)
1	goethite (FeOOH)	4.25	4.27	0.4683
2	hematite (Fe_2O_3)	5.27	5.28	0.1893
3	magnetite (Fe_3O_4)	5.17	5.20	0.5769
4	aluminum oxide (Al_2O_3)	3.95	3.98	0.7537
5	aluminum hydroxide ($Al(OH)_3$)	2.42	2.39	−1.2552
6	titanium dioxide (TiO_2)	4.12	4.24	2.8301
7	lanthanum oxide (La_2O_3)	6.51	6.56	0.7621
8	lanthanum hydroxide ($La(OH)_3$)	4.28	4.46	4.0358
9	stannic oxide (SnO_2)	6.95	6.99	0.5722
10	silver oxide (Ag_2O)	7.14	7.31	2.3255
11	zirconium oxide (ZrO_2)	5.68	5.82	2.4054
12	tin oxide (SnO)	6.45	6.44	−0.1552
13	zinc oxide (ZnO)	5.61	5.67	1.0582
14	ferrous oxide (FeO)	5.74	5.87	2.2146
15	silicon oxide (SiO_2)	2.65	2.64	−0.3787

First, calculations were performed for the FeOOH adsorbent toward arsenic (H_2AsO_4) at pH 3 to validate the computational framework. Figure 3 displays the structures after performing a sorption task with red dots above FeOOH, indicating that arsenic was successfully adsorbed on its surface.

An adsorption capacity of 78.6 mg/g was obtained from sorption calculations, which was comparable to the literature-reported value of 76 mg/g at the same pH value of 3 and yielded a low percentage error of less than 10%.[33] Considering this as a benchmark, a sorption simulation was performed for all other adsorbents during screening.

After the sorption simulation, few graphs are obtained explaining the sorption sites (Figure 4), sorption loading (Figure 5) to calculate the adsorption capacity, and energy

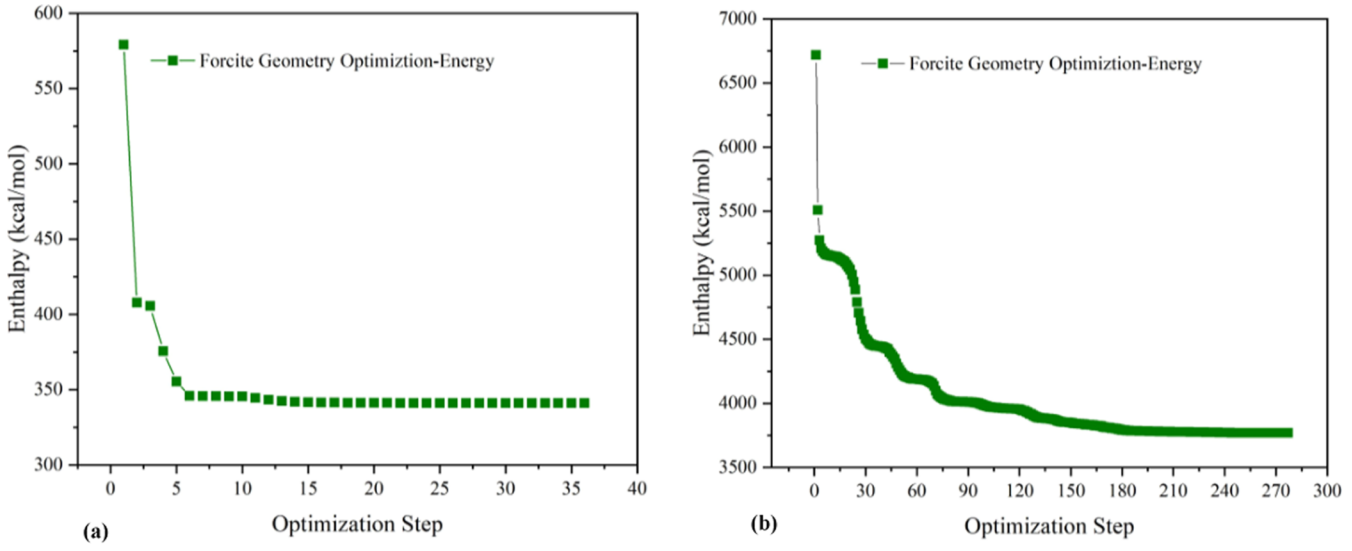

Figure 1. Graphs for Forcite geometry optimization: (a) FeOOH and (b) $Al(OH)_3$.

https://doi.org/10.1021/acsomega.3c07014
ACS Omega 2023, 8, 48130−48144

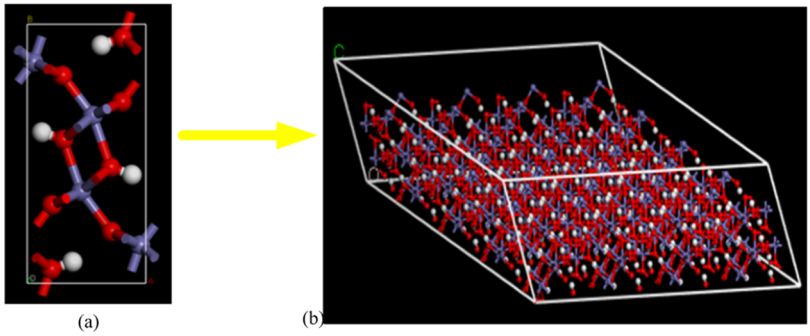

Figure 2. Structure of FeOOH after (a) importing and (b) building the surface.

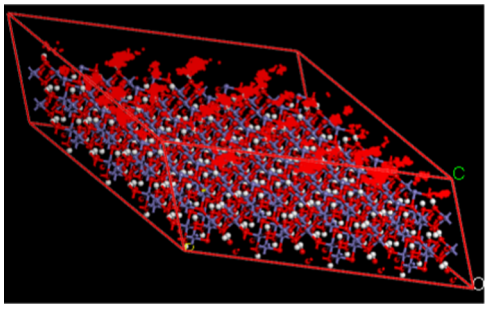

Figure 3. Arsenic adsorption on FeOOH at a pH range of 3−7.

values (Figure 6) involved in the sorption phenomenon. The maximum adsorption capacity was obtained for $Al(OH)_3$ (197 mg/g). The energy distribution graph for FeOOH and $Al(OH)_3$ showed peaks at −6.5 and −14.5 kcal/mol, respectively, as given in Figure 4a,b, respectively, exhibiting the largest number of available sorption sites at these locations. This supported the sorption capacity, since the higher peaks observed for the energy distribution indicated the strongest interaction between the arsenic species and the adsorbent. The energy distribution spectrum was wider for $Al(OH)_3$, indicating more site availability for $Al(OH)_3$, and a more negative value indicated a stronger interaction, too, thus having more adsorption capacity than FeOOH.

The energy graph results indicated that van der Waals energy was the major sorption energy, while electrostatic energy recorded the least contribution, as illustrated in Figure 6, and the adsorption separation mainly depends on van der Waals interaction and electrostatic interaction.[26] According to the energy graph (Figure 6) for sorption, it was observed that the dominant energies for sorption were van der Waals and intermolecular interactions for both FeOOH and $Al(OH)_3$, as displayed in Figure 6a,b, respectively. van der Waals energy stabilized the sorption process, while intermolecular energy promoted the interaction of arsenic species with the adsorbent.[94] The graph for loading per cell is given in Figure 5. The amount of arsenic adsorbed on the adsorbent surface was indicated, while the average loading was further used for calculating the adsorption capacity by involving the volume of the adsorbent, as given in eq 1. The average loadings for FeOOH and $Al(OH)_3$ were 5.9 and 49.1, respectively (as displayed in Figure 5b,a, respectively). The loading graph indicated the number of sorbent species that were in contact with the adsorbent at a given temperature and fugacity.[38] The greater the loading, the higher the adsorption capacity of the adsorbent, which indicated the suitability for arsenic removal from water. The calculated adsorption capacity for all of the adsorbents is given in Table 4.

Arsenic loading on $Al(OH)_3$ is illustrated in the graph given in Figure 5a. It was consistent with the reported literature that aluminum-based water treatment residuals have more potential

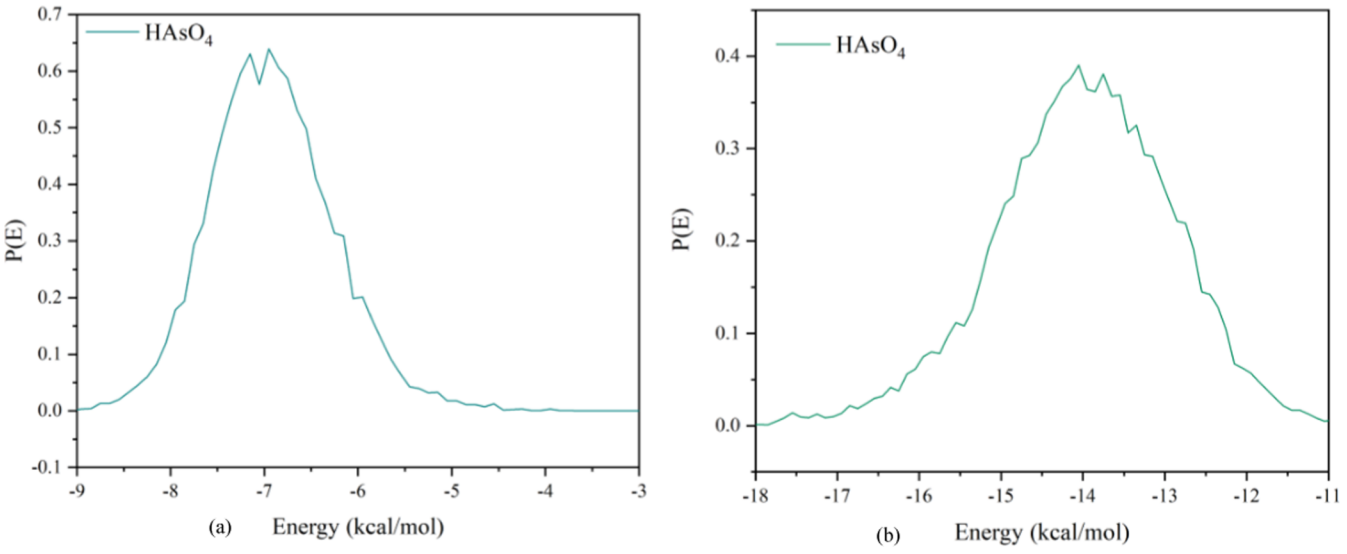

Figure 4. Energy distribution graph for (a) FeOOH and (b) $Al(OH)_3$.

https://doi.org/10.1021/acsomega.3c07014
ACS Omega 2023, 8, 48130−48144

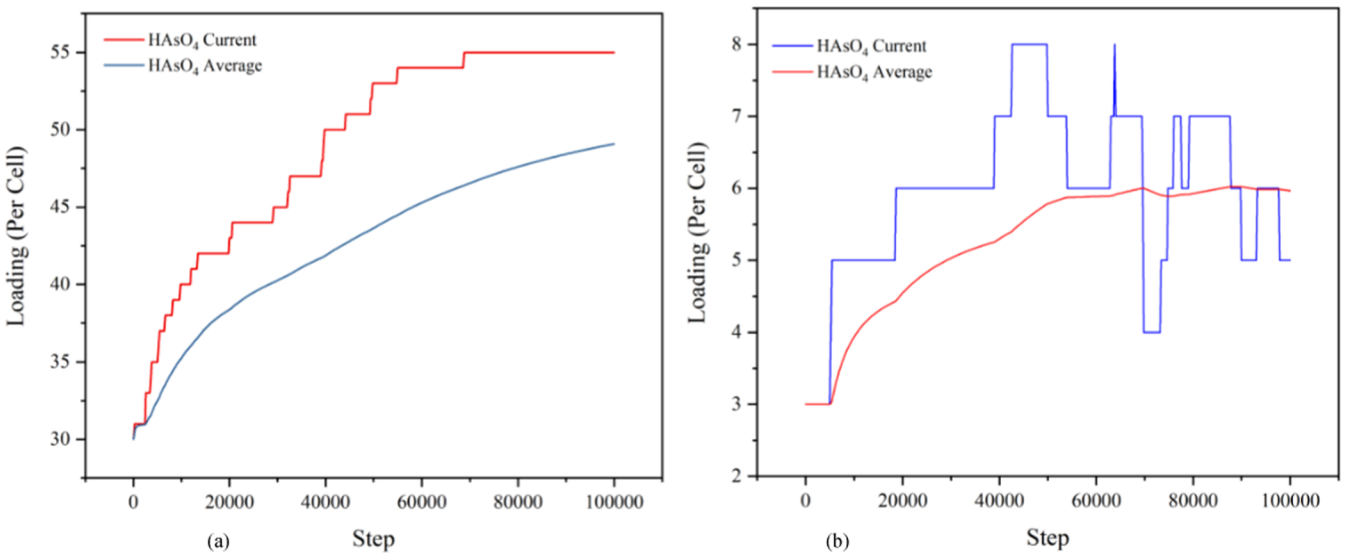

Figure 5. Illustration of arsenic loading per cell of adsorbent for (a) $Al(OH)_3$ and (b) FeOOH.

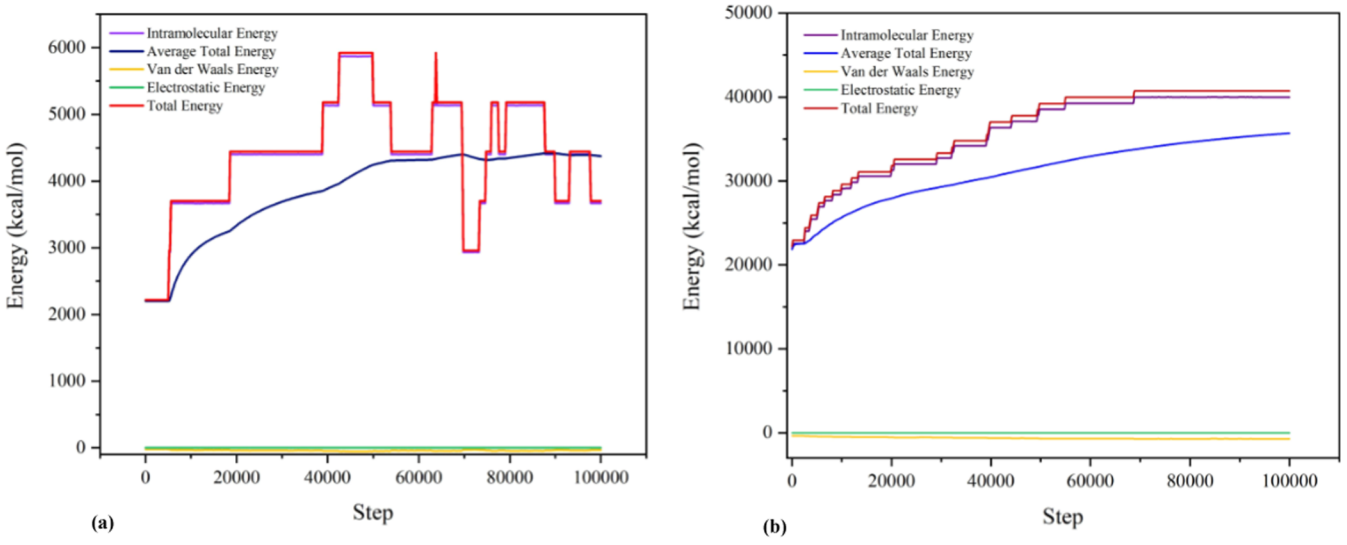

Figure 6. Illustration of energy values obtained from simulations for sorption of arsenic for (a) FeOOH and (b) $Al(OH)_3$.

Table 4. Calculated Adsorption Capacities for All Adsorbents

sr. no.	metal oxide/hydroxide	adsorption capacity (mg/g)
1	FeOOH	73.636
2	Fe_2O_3	30.417
3	Fe_3O_4	14.17
4	Al_2O_3	16.7
5	TiO_2	43.14
6	$Al(OH)_3$	197.24
7	ZrO_2	7.9933
8	Ag_2O	6.361
9	La_2O_3	3.59
10	SnO_2	42.75
11	FeO	0
12	ZnO	11.7
13	SiO_2	64.8
14	SnO	11.135
15	$La(OH)_3$	151.07

than iron-based water treatment residuals and should be used for arsenic removal from water.[95] Nonetheless, most of the literature on arsenic removal was still focused on iron-based adsorbents. The second highest adsorption capacity was obtained by $La(OH)_3$, which showed great potential for arsenic removal, suggesting that metal hydroxides are more effective in treating toxic water than metal oxides. Previously, in a comparative study for phosphate removal from wastewater using metal oxides and hydroxides, it was reported that metal hydroxides were better adsorbents due to the excessive hydroxyl groups on the surface.[96]

Most of the selected metal oxides and hydroxides showed good potential for arsenic removal from water, and among these selected adsorbents, the top 7 adsorbents on the basis of adsorption capacity for arsenic removal are $Al(OH)_3$, $La(OH)_3$, FeOOH, SiO_2, TiO_2, SnO_2, and Fe_2O_3 with adsorption capacities of 197, 151, 73.6, 64.8, 43.14, 42.7, and 30.4 mg/g, respectively. Currently, SnO_2 is not typically used for arsenic removal from water but rather employed to eliminate other heavy metals like cadmium and lead from water and should be

https://doi.org/10.1021/acsomega.3c07014
ACS Omega 2023, 8, 48130−48144

given consideration to explore its viability in later studies.[97] The order of the sorbents according to their sorption capacity values was $Al(OH)_3$ > $La(OH)_3$ > FeOOH > SiO_2 > TiO_2 > SnO_2 > Fe_2O_3 > Al_2O_3 > Fe_3O_4 > SnO > ZnO > ZrO_2 > Ag_2O > La_2O_3 > FeO.

3.2.1. Effect of pH. The effect of pH for arsenic removal from water at a standard temperature of 298 K and 100 kPa pressure was studied, and the result demonstrated that arsenic removal increased in a slightly acidic medium to neutral while decreasing in a basic medium.[28,98] The overall effect of pH for all adsorbents is depicted in Figure 7.

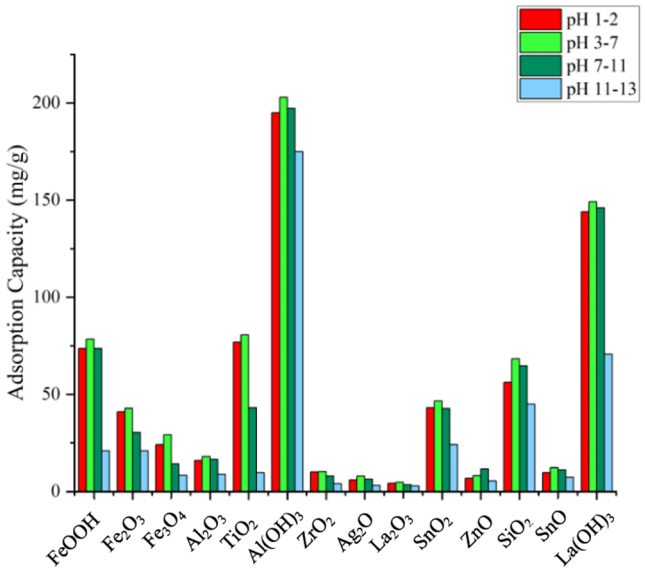

Figure 7. Effect of the pH for all adsorbents.

Variations in pH would modify the surface charge of the adsorbent and the forms of the arsenic species, which would affect the adsorption of arsenic.[99] The positive charge density of adsorbents decreases at very low pH values, and thus, the rate of arsenate adsorption decreases. When the pH is high (greater than 8), the surface of adsorbents is negatively charged, and Coulombic repulsions between the negatively charged ion and the negatively charged surface considerably reduce the rate of arsenate adsorption.[10] Furthermore, for alkaline speciation, the depression of negative charge occurs, which reduces the adsorption capacity due to negative surface charge.[100]

The effect of pH can be explained in terms of point of zero charge (PZC), which is a crucial variable in governing the adsorption process. It refers to the pH at which the surface charge of the adsorbent is neutral, meaning that it has no net positive or negative charge. The surface of the adsorbent will be positively charged when the pH of a solution is below the PZC,[101] and vice versa.[102] It was observed that when the pH was less than point zero charge (pH_{pzc}), a strong electrostatic attraction existed, while for pH greater than pH_{pzc}, the negatively charged adsorbent would have electrostatic repulsion, thus reducing the adsorption capacity.[103,104] In this context, a negatively charged surface layer on the sorbents did not promote anionic molecule adsorption because of repulsive forces. On the contrary, the process with low pH involved an increase in H^+ ionic strength, and by attracting H^+ ions, the surface of the sorbents pursued a positive charge. Due to the positively charged adsorbent surfaces at low pH, an electrostatic attraction was developed between the positively charged adsorbate molecules and the anionic molecule, leading to full sorption. As the pH increased, the number of negatively charged sites increased while the number of positively charged sites decreased.[25] As(V) existed in the form of H_3AsO_4, $H_2AsO_4^{-1}$, $HAsO_4^{-2}$, and AsO_4^{-3} at pH 1, 3, 7, and 11, respectively.[86] So, under acidic conditions, there were more H^+ ions, and as the pH increased, negatively charged ions also gradually increased.

It was noted that the average total energy was higher for sorption with pH between 3 and 7 compared to other ranges. In general, the adsorption capacities were consistent with the trend in the average total energies, which were 33210.33, 64899.28, 35703.19, and 30344.01 kcal/mol, respectively, for pH ranges of 1 to 2, 3 to 7, 7 to 11, and 11 onward for $Al(OH)_3$. The same trend was observed for all other adsorbents, whereby the adsorption capacity was lesser in strongly acidic and basic media. It was also noticed that the average total energy for Fe_2O_3 at pH 3−7 was relatively higher, which indicated good interaction between arsenic and adsorbent Fe_2O_3 for that range. These results were supported by the experimental literature by showing a similar trend for the same pH range.[105] Previously, the effect of pH was studied for compounds that included iron oxides and aluminum oxide.

In a study that involved arsenic removal from water using Fe_2O_3, the adsorption capacity decreased at pH greater than 6.[27] In the study, it was reported that with increasing pH, the arsenate species did not get adsorbed on Fe_2O_3 due to a negative surface charge, Coulombic repulsion, and interaction of the arsenate species with the surface sites of Fe_2O_3 that are inhabited by hydrogen ions, thus showing a decrease in adsorption capacity with the increase in pH, which was the same observations as obtained from this simulation work. For TiO_2, the adsorption capacity dropped drastically, and in a previous study, it was reported that the repulsive forces between oxyanions and the negatively charged surface of TiO_2 caused a decline in adsorption capacity, since As(V) existed as AsO_4^{-3} at pH greater than 11, which increased the repulsion that halted the adsorption phenomenon. All selected adsorbents contained oxygen and, hence, encountered repulsion that decreased the interaction energy and hence the adsorption capacity. For all of the adsorbents, adsorption capacity decreased for pH greater than 11.

3.2.2. Effect of Temperature. The effect of temperature for arsenic removal from water was studied at a range of 281.15 to 321.15 K at pH 7 and 100 kPa pressure. The results revealed that removal increased at lower temperatures and gradually decreased with an increase in temperature. In the literature, it is mentioned that due to the high activation energy in chemical adsorption, the extent of adsorption initially increases and then decreases as the temperature increases.[106] The overall effect of the temperature for all adsorbents is depicted in Figure 8.

This can be explained by the energy graph obtained for sorption at each temperature, whereby it was observed that the interaction energy between the sorbent and the sorbate decreased at higher temperatures.[94] For instance, the energy values for FeOOH at 281.15, 291.15, 301.15, 311.15, and 321.15 K were 5564.915, 5394.198, 3669.215, 3173.903, and 2073.831 kcal/mol, respectively. A similar trend had been reported in the literature, in which the removal increased at the initial temperature and then gradually decreased when the temperature increased.[105] Pillai et al. reported the same trend for arsenic removal from water with the reason that with the

https://doi.org/10.1021/acsomega.3c07014
ACS Omega 2023, 8, 48130−48144

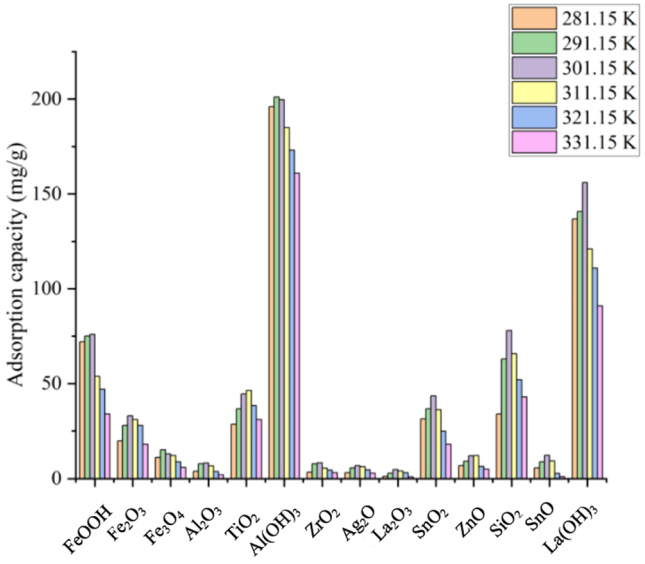

Figure 8. Effect of temperature on adsorption.

increase in temperature, the randomness of arsenic ions increases, which reduces arsenic adsorption.[105] Moreover, according to certain reports, ions' mobility increases as the temperature increases. When the temperature increases above 303.15 K, surface complexation and electrostatic interactions may become less intense.[107]

3.2.3. Effect of Pressure. Previous research work did not focus on studying the effect of pressure on adsorption. The sorption calculations were performed for the pressure range of 100−300 kPa. The results demonstrated that the removal of arsenic increased with increasing pressure to a certain range. The overall trend of pressure for adsorption of arsenic is given in Figure 9.

For example, the interaction energies of FeOOH at 100, 150, 200, 250, 300, and 350 kPa were 4951.20, 6867.88, 8377.17, 9061.88, 8787.07, and 8190.47 kcal/mol, respectively. This may be because at low pressures, the surface of the adsorbent may not be fully covered by adsorbed molecules. As

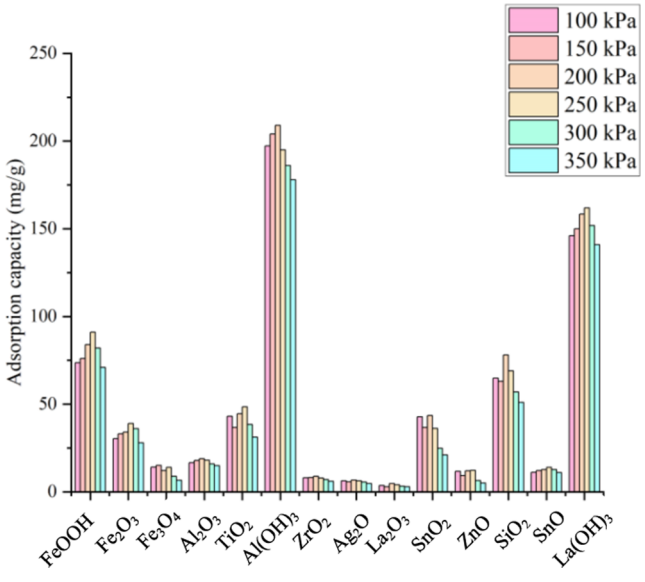

Figure 9. Effect of pressure on adsorption.

the pressure increases, more molecules are available for adsorption, leading to increased surface coverage and a higher overall adsorption capacity. The energy value results also revealed that pressure promoted the interaction energy and adsorption capacity. Previously, it has been discussed for factors affecting adsorption in physical chemistry and reported that adsorption is directly proportional to the pressure over a limited range of pressure, as at higher pressure, the adsorption phenomenon becomes independent of pressure.[106,108] Moreover, there are a finite number of adsorption sites on the solid surface where sorbent molecules can bind. The rate of adsorption initially increases as the pressure is elevated because more molecules interact with the surface. As a result, the rate of adsorption increases linearly as the pressure increases. However, eventually, the number of adsorption sites will be saturated, and no more adsorptions can take place there, so the pressure will have no further impact on the rate of adsorption. The degree of adsorption will therefore be independent of pressure after a certain point.[107]

3.3. Empirical Modeling Results. The empirical modeling calculations were performed for the top 3 screened adsorbents, i.e., $Al(OH)_3$ (as R1), $La(OH)_3$ (as R2), and FeOOH (as R3). The values of the combinations of the three independent variables (A: pH, B: temperature, and C: pressure) and the results of the response (adsorption capacity) were provided for the CCD actual design to conduct the analysis. The ANOVA was performed, and Table 5 displays the F- and p-values for the impacts of operating variables toward the adsorption capacities of $Al(OH)_3$ (as R1), $La(OH)_3$ (as R2), and FeOOH (as R3).

The F-values for R1, R2, and R3 were 13.01, 11.7, and 24.48, respectively, implying that the model is significant. The *P*-values less than 0.0500 indicate that model terms were significant. For R1, the terms A, B, A^2, and B^2 were significant model terms. For R2, A and B were significant model terms, while for R3, A, B, C, AB, and A^2 were significant model terms. The R^2 values for R1, R2, and R3 are 0.921, 0.676, and 0.956 with adequate precision values of 13.3, 12.7, and 18.3, respectively. Adequate precision measures the signal-to-noise ratio.[49] A ratio of >4 is desirable. Herein, the ratio obtained for all models was greater than 4, which indicates an adequate signal. The predicted R^2 for all responses was in reasonable agreement with the adjusted R^2. The R^2 value and adequate precision values are given in Table 6.

The three corresponding equations for R1, R2, and R3 as given in eqs 2−4 in terms of actual factors obtained from CCD, respectively. The data points were tested with the range of operating variables, and it was observed that adsorption capacity was mainly affected by the pH value. These equations were validated using some simulation results that were not a part of the regression model, and the error was less than 10%, as demonstrated in Table 7.

$$\begin{aligned} R1 = {} & -739.56525 - 1.92890 \times pH + 6.42582 \\ & \times temperature + 0.063769 \times pressure \\ & + 0.013644 \times pH \times temperature + 0.001628 \times pH \\ & \times pressure + 0.000584 \times temperature \times pressure \\ & - 0.252157 \times pH^2 - 0.011245 \times temperature^2 \\ & - 0.000524 \times pressure^2 \end{aligned} \quad (2)$$

https://doi.org/10.1021/acsomega.3c07014
ACS Omega 2023, 8, 48130−48144

Table 5. ANOVA for Evaluation of the Model

source	sum of squares	degree of freedom	mean square	F-value	*p*-value	
			R1			
model	2092.81	9	232.53	13.01	0.0002	significant
A: pH	246.80	1	246.80	13.81	0.0040	
B: temperature	262.96	1	262.96	14.71	0.0033	
C: pressure	64.11	1	64.11	3.59	0.0875	
AB	24.00	1	24.00	1.34	0.2736	
AC	14.51	1	14.51	0.8119	0.3888	
BC	27.54	1	27.54	1.54	0.2429	
A^2	273.22	1	273.22	15.28	0.0029	
B^2	108.77	1	108.77	6.08	0.0333	
C^2	85.48	1	85.48	4.78	0.0536	
residual	178.77	10	17.88			
			R2			
model	12543.69	3	4181.23	11.17	0.0003	significant
A: pH	5386.26	1	5386.26	14.39	0.0016	
B: temperature	5306.79	1	5306.79	14.18	0.0017	
C: pressure	957.41	1	957.41	2.56	0.1293	
residual	5987.50	16	374.22			
			R3			
model	8802.40	9	978.04	24.48	<0.0001	significant
A: pH	3112.18	1	3112.18	77.89	<0.0001	
B: temperature	1582.99	1	1582.99	39.62	<0.0001	
C: pressure	676.21	1	676.21	16.92	0.0021	
AB	233.11	1	233.11	5.83	0.0363	
AC	4.49	1	4.49	0.1124	0.7444	
BC	188.40	1	188.40	4.72	0.0550	
A^2	505.00	1	505.00	12.64	0.0052	
B^2	1.08	1	1.08	0.0269	0.8729	
C^2	99.33	1	99.33	2.49	0.1459	
residual	399.57	10	39.96			

Table 6. Statistical Fit of Models

response	R^2 (*R*-square)	adeq precision
R1	0.9213	13.3869
R2	0.6769	12.7033
R3	0.9566	18.3942

$$R2 = 440.76323 - 3.80664 \times pH - 0.963364 \times temperature + 0.064205 \times pressure \quad (3)$$

$$R3 = 130.52087 + 14.36459 \times pH + 0.067536 \times temperature - 0.161222 \times pressure - 0.042527 \times pH \times temperature + 0.000906 \times pH \times pressure + 0.001528 \times temperature \times pressure - 0.342816 \times pH^2 - 0.001119 \times temperature^2 - 0.000565 \times pressure^2 \quad (4)$$

The two most significant interactive effects (pH and temperature) of R1, R2, and R3 are illustrated as three-dimensional response surface plots in Figure 10.

Representative response surface plots showed the effect of the pH and temperature on arsenic removal. The arsenic removal increased with the increase in pH and had a direct relation with adsorption capacity. Temperature also has a linear inverse relation after 301 K with adsorption capacity, while it has a direct relation with adsorption capacity to a certain extent.

Table 7. Equations Validation Obtained after Calculations

	pH	temperature (°K)	pressure (kPa)	simulation result	equation results	error (%)
R1	7	298	100	197.2	199.0	9
	7	298	150	204.1	204.9	1
R2	7	298	100	146	133.5	8
	7	298	150	150	136.9	8.8
R3	7	298	100	73.6	71	3
	7	298	150	76	78.6	3

4. CONCLUSIONS

Currently, the molecular simulations are confined to very few adsorbents for arsenic removal from water, which do not specify the best adsorbent to remove arsenic from water. This research aimed to study 15 adsorbents by using a molecular simulation approach via molecular dynamics and Monte Carlo simulations to screen various metal oxides for sorption ability. The order of the sorbents according to their adsorption capacity values was $Al(OH)_3$ > $La(OH)_3$ > FeOOH > SiO_2 > TiO_2 > SnO_2 > Fe_2O_3 > Al_2O_3 > Fe_3O_4 > SnO > ZnO > ZrO_2 > Ag_2O > La_2O_3 > FeO. $Al(OH)_3$, FeOOH, and $La_2(OH)_3$ had the maximum adsorption capacities of 197, 73.6, and 151 mg/g, respectively. Other potential adsorbents were SiO_2, TiO_2, SnO_2, and Fe_2O_3. SnO_2, which is a metal oxide that has not been used to treat arsenic-contaminated water but has been used to remove cadmium and lead from water, showed a

https://doi.org/10.1021/acsomega.3c07014
ACS Omega 2023, 8, 48130−48144

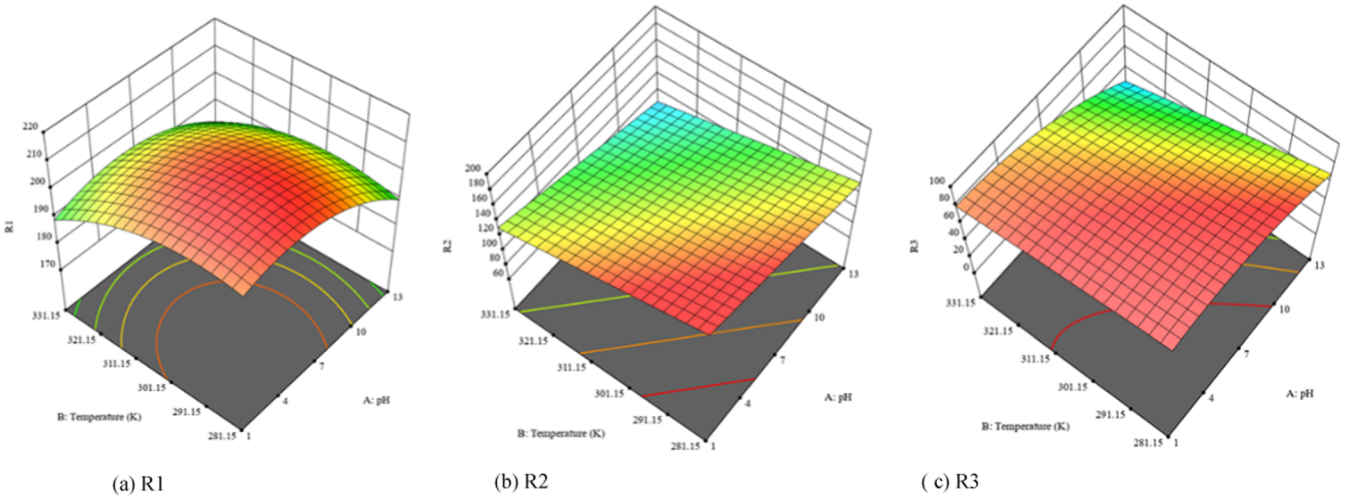

(a) R1 (b) R2 (c) R3

Figure 10. Response surface plots for (a) R1, (b) R2, and (c) R3.

good adsorption ability for arsenic removal and should be used as an adsorbent in countries where it is abundantly present. This work also revealed that $Al(OH)_3$ and $La(OH)_3$ demonstrated high adsorption capacities and ability to remove arsenic from water, which should be further investigated as viable adsorbents for this purpose apart from using conventional iron oxides. The effect of operating variables was also determined, and results showed that the arsenic removal process was most affected by pH, then temperature, and last by pressure. In the future, it will be better to do the screening of adsorbents for other heavy metals such as mercury with consideration of the impact of operating variables. As an outcome of this research work, it is recommended that while designing a plant for arsenic removal from water, the effect of operating variables should be considered, as they affect the adsorption phenomenon significantly, and the results reported herein can also provide guidelines for other adsorbents and adsorption processes.

AUTHOR INFORMATION

Corresponding Author

Serene Sow Mun Lock − *CO2 Research Centre (CO2RES), Universiti Teknologi PETRONAS, 32610 Seri Iskandar, Perak, Malaysia; Department of Chemical Engineering, Universiti Teknologi PETRONAS, 32610 Seri Iskandar, Perak, Malaysia;* orcid.org/0000-0003-2285-0308; Email: sowmun.lock@utp.edu.my

Authors

Noor E. Hira − *CO2 Research Centre (CO2RES), Universiti Teknologi PETRONAS, 32610 Seri Iskandar, Perak, Malaysia; Department of Chemical Engineering, Universiti Teknologi PETRONAS, 32610 Seri Iskandar, Perak, Malaysia*

Ushtar Arshad − *CO2 Research Centre (CO2RES), Universiti Teknologi PETRONAS, 32610 Seri Iskandar, Perak, Malaysia; Department of Chemical Engineering, Universiti Teknologi PETRONAS, 32610 Seri Iskandar, Perak, Malaysia*

Khadija Asif − *CO2 Research Centre (CO2RES), Universiti Teknologi PETRONAS, 32610 Seri Iskandar, Perak, Malaysia; Department of Chemical Engineering, Universiti Teknologi PETRONAS, 32610 Seri Iskandar, Perak, Malaysia*

Farman Ullah − *Centre of Innovative Nanostructures & Nanodevices, Universiti Teknologi PETRONAS, 32610 Seri Iskandar, Perak, Malaysia*

Abid Salam Farooqi − *CO2 Research Centre (CO2RES), Universiti Teknologi PETRONAS, 32610 Seri Iskandar, Perak, Malaysia; Centre of Innovative Nanostructures & Nanodevices, Universiti Teknologi PETRONAS, 32610 Seri Iskandar, Perak, Malaysia*

Chung Loong Yiin − *Department of Chemical Engineering and Energy Sustainability, Faculty of Engineering, Universiti Malaysia Sarawak (UNIMAS), 94300 Kota Samarahan, Sarawak, Malaysia; Institute of Sustainable and Renewable Energy (ISuRE), Universiti Malaysia Sarawak (UNIMAS), 94300 Kota Samarahan, Sarawak, Malaysia*

Bridgid Lai Fui Chin − *Department of Chemical and Energy Engineering, Faculty of Engineering and Science and Energy and Environment Research Cluster, Faculty of Engineering and Science, Curtin University Malaysia, 98009 Miri, Sarawak, Malaysia*

Zill e Huma − *University of the Punjab, Lahore 54590 Punjab, Pakistan*

Complete contact information is available at: https://pubs.acs.org/10.1021/acsomega.3c07014

Notes

The authors declare no competing financial interest.

ACKNOWLEDGMENTS

This research was funded by the CO_2 Research Centre (CO2RES), Universiti Teknologi PETRONAS (Cost Center: 015LB0-081), and Yayasan Universiti Teknologi PETRONAS (Cost Center: 015LC0-498).

REFERENCES

(1) Dye, C.; Reeder, J. C.; Terry, R. F. Research for Universal Health Coverage. *Sci. Transl. Med.* **2013**, *5* (199), No. 199ed13.

(2) Tchounwou, P. B.; Yedjou, C. G.; Patlolla, A. K.; Sutton, D. J. *Molecular, Clinical and Environmental Toxicicology Volume 3: Environmental Toxicology*; Springer: Basel, 2012; Vol. *101* DOI: 10.1007/978-3-7643-8340-4_6.

(3) Soomro, Z. A.; Khokhar, M. I. A.; Hussain, W.; Hussain, M.*Drinking Water Quality Challenges in Pakistan*, Pakistan Council of Research in Water Resources, Lahore, 2011; pp 17−28.
(4) Xia, C.; Joo, S. W.; Hojjati-Najafabadi, A.; Xie, H.; Wu, Y.; Mashifana, T.; Vasseghian, Y. Latest Advances in Layered Covalent Organic Frameworks for Water and Wastewater Treatment. *Chemosphere* **2023**, *329* (April), No. 138580.
(5) Singh, R.; Singh, S.; Parihar, P.; Singh, V. P.; Prasad, S. M. Arsenic Contamination, Consequences and Remediation Techniques: A Review. In *Ecotoxicology and Environmental Safety*; Academic Press, February 1, 2015; pp 247−270 DOI: 10.1016/j.ecoenv.2014.10.009.
(6) Fakhar, A.; Gul, B.; Gurmani, A. R.; Khan, S. M.; Ali, S.; Sultan, T.; Chaudhary, H. J.; Rafique, M.; Rizwan, M. Heavy Metal Remediation and Resistance Mechanism of Aeromonas, Bacillus, and Pseudomonas: A Review. *Crit. Rev. Environ. Sci. Technol.* **2022**, *52* (11), 1868−1914.
(7) Kurganskaya, I.; Niazi, N. K.; Luttge, A. A Modeling Approach for Unveiling Adsorption of Toxic Ions on Iron Oxide Nanocrystals. *J. Hazard. Mater.* **2021**, *417*, No. 126005.
(8) Sakai, N.; Alsaad, Z.; Thuong, N. T.; Shiota, K.; Yoneda, M.; Ali Mohd, M. Source Profiling of Arsenic and Heavy Metals in the Selangor River Basin and Their Maternal and Cord Blood Levels in Selangor State, Malaysia. *Chemosphere* **2017**, *184*, 857−865.
(9) Huang, Y.; Yang, J. K.; Keller, A. A. Removal of Arsenic and Phosphate from Aqueous Solution by Metal (Hydr-)Oxide Coated Sand. *ACS Sustainable Chem. Eng.* **2014**, *2* (5), 1128−1138.
(10) Mamindy-Pajany, Y.; Hurel, C.; Marmier, N.; Roméo, M. Arsenic (V) Adsorption from Aqueous Solution onto Goethite, Hematite, Magnetite and Zero-Valent Iron: Effects of PH, Concentration and Reversibility. *Desalination* **2011**, *281* (1), 93−99.
(11) Choong, T. S. Y.; Chuah, T. G.; Robiah, Y.; Gregory Koay, F. L.; Azni, I. Arsenic Toxicity, Health Hazards and Removal Techniques from Water: An Overview. *Desalination* **2007**, *217* (1−3), 139−166.
(12) Yoon, K.; Cho, D. W.; Kwon, G.; Rinklebe, J.; Wang, H.; Song, H. (2023). Practical Approach of As (V) Adsorption by Fabricating Biochar with Low Basicity from FeCl3 and Lignin. *Chemosphere* **2023**, *329*, 138665.
(13) Jha, S. K.; Mishra, V. K.; Damodaran, T.; Sharma, D. K.; Kumar, P. Arsenic in the Groundwater: Occurrence, Toxicological Activities, and Remedies. *J. Environ. Sci. Health, Part C: Environ. Carcinog. Ecotoxicol. Rev.* **2017**, *35* (2), 84−103.
(14) Palma-Lara, I.; Martínez-Castillo, M.; Quintana-Pérez, J. C.; Arellano-Mendoza, M. G.; Tamay-Cach, F.; Valenzuela-Limón, O. L.; García-Montalvo, E. A.; Hernández-Zavala, A. Arsenic Exposure: A Public Health Problem Leading to Several Cancers. *Regul. Toxicol. Pharmacol.* **2020**, *110* (June 2019), No. 104539.
(15) Nicomel, N. R.; Leus, K.; Folens, K.; Van Der Voort, P.; Du Laing, G. Technologies for Arsenic Removal from Water: Current Status and Future Perspectives. *Int. J. Environ. Res. Public Health* **2016**, *13* (1), No. 62.
(16) Yin, H.; Kong, M.; Gu, X.; Chen, H. Removal of Arsenic from Water by Porous Charred Granulated Attapulgite-Supported Hydrated Iron Oxide in Bath and Column Modes. *J. Cleaner Prod.* **2017**, *166*, 88−97.
(17) Mukherjee, S.; Kumar, A. A.; Sudhakar, C.; Kumar, R.; Ahuja, T.; Mondal, B.; Srikrishnarka, P.; Philip, L.; Pradeep, T. Sustainable and Affordable Composites Built Using Microstructures Performing Better than Nanostructures for Arsenic Removal. *ACS Sustainable Chem. Eng.* **2019**, *7* (3), 3222−3233.
(18) Ahmad, A.; Bhattacharya, P. Environmental Arsenic in a Changing World. *Groundw. Sustainable Dev.* **2019**, *8* (October 2018), 169−171.
(19) Mondal, P.; Bhowmick, S.; Chatterjee, D.; Figoli, A.; Van der Bruggen, B. Remediation of Inorganic Arsenic in Groundwater for Safe Water Supply: A Critical Assessment of Technological Solutions. *Chemosphere* **2013**, *92* (2), 157−170.
(20) Hira, N. e.; Lock, S. S. M.; Shoparwe, N. F.; Lock, I. S. M.; Lim, L. G.; Yiin, C. L.; Chan, Y. H.; Hassam, M. Review of Adsorption Studies for Contaminant Removal from Wastewater Using Molecular Simulation. *Sustainability* **2023**, *15* (2), 1−27.
(21) Rashid, R.; Shafiq, I.; Akhter, P.; et al. A State-of-the-Art Review on Wastewater Treatment Techniques: The Effectiveness of Adsorption Method. *Env. Sci. Pollut Res.* **2021**, *28*, 9050−9066.
(22) Rathi, B. S.; Kumar, P. S. Application of Adsorption Process for Effective Removal of Emerging Contaminants from Water and Wastewater. *Environ. Pollut.* **2021**, *280*, No. 116995.
(23) Bobade, V.; Eshtiaghi, N.; Eshtiagi, N. In *Heavy Metals Removal from Wastewater by Adsorption Process: A Review*, Pap. no. APCChE 2015 Congr. Inc. Chemeca, 2015.
(24) Etienne, H. P.; Hounguè, J. H.; Mensah, M. T. A. K.; Michel. A First Principle Evaluation of the Adsorption Mechanism and Stability of Volatile Organic Compounds into NaY Zeolite. *Z. Kristallogr. - Cryst. Mater.* **2019**, *234* (7−8), 469−482.
(25) Tran, N. V.; Tieu, A. K.; Zhu, H.; Huong, T. T. Ta.; Thi, D. Ta.; Le, H. M. First-Principles Study of the Adsorption and Depolymerization Mechanisms of Sodium Silicate on Iron Surfaces at High Temperature. *J. Phys. Chem. C* **2018**, *122* (36), 20827−20840.
(26) Alka, S.; Shahir, S.; Ibrahim, N.; Ndejiko, M. J.; Vo, D. V. N.; Manan, F. A. Arsenic Removal Technologies and Future Trends: A Mini Review. *J. Cleaner Prod.* **2021**, *278*, No. 123805.
(27) Jeong, Y.; Fan, M.; Singh, S.; Chuang, C. L.; Saha, B.; Hans van Leeuwen, J. Evaluation of Iron Oxide and Aluminum Oxide as Potential Arsenic(V) Adsorbents. *Chem. Eng. Process. Process Intensif.* **2007**, *46* (10), 1030−1039.
(28) Gallegos-Garcia, M.; Ramírez-Muñiz, K.; Song, S. Arsenic Removal from Water by Adsorption Using Iron Oxide Minerals as Adsorbents: A Review. *Miner. Process. Extr. Metall. Rev.* **2012**, *33* (5), 301−315.
(29) Chen, L.; Xin, H.; Fang, Y.; Zhang, C.; Zhang, F.; Cao, X.; Zhang, C.; Li, X. Application of Metal Oxide Heterostructures in Arsenic Removal from Contaminated Water. *J. Nanomater.* **2014**, *2014*, No. 793610.
(30) Gulledge, J. H.; O'Connor, J. T. Removal of Arsenic (V) from Water by Adsorption on Aluminum and Ferric Hydroxides. *J./Am. Water Work. Assoc.* **1973**, *65* (8), 548−552.
(31) Tang, W.; Li, Q.; Gao, S.; Shang, J. K. Arsenic (III,V) Removal from Aqueous Solution by Ultrafine α-Fe2O3 Nanoparticles Synthesized from Solvent Thermal Method. *J. Hazard. Mater.* **2011**, *192* (1), 131−138.
(32) Mamindy-Pajany, Y.; Hurel, C.; Marmier, N.; Roméo, M. Arsenic Adsorption onto Hematite and Goethite. *Comptes Rendus Chim.* **2009**, *12* (8), 876−881.
(33) Ghosh, M. K.; Gérrard Eddy Jai Poinern, G. E. J.; Issa, T. B.; S, P. Arsenic Adsorption on Goethite Nanoparticles Produced through Hydrazine Sulfate Assisted Synthesis Method. *Korean J. Chem. Eng.* **2012**, *29* (1), 95−102.
(34) Hao, L.; Liu, M.; Wang, N.; Li, G. A Critical Review on Arsenic Removal from Water Using Iron-Based Adsorbents. *RSC Adv.* **2018**, *8* (69), 39545−39560.
(35) Ulatowska, J. Adsorption Behaviour of As(III) onto Synthetic Iron-Based Minerals: A Comparative Study of Akaganeite, Goethite and Magnetite. *Physicochem. Probl. Miner. Process* **2022**, *58* (2), No. 144818.
(36) Xiong, H.; Hu, D.; Shi, K.; Zhu, S.; Xu, Y. Adsorptive Removal of Arsenic Ions from Contaminated Water Using Low-Cost Schwertmannites and Akaganéites. *Mater. Chem. Phys.* **2023**, *297* (October 2022), No. 127411.
(37) Zeng, K.; Hachem, K.; Kuznetsova, M.; Chupradit, S.; Su, C. H.; Nguyen, H. C.; El-Shafay, A. S. Molecular Dynamic Simulation and Artificial Intelligence of Lead Ions Removal from Aqueous Solution Using Magnetic-Ash-Graphene Oxide Nanocomposite. *J. Mol. Liq.* **2022**, *347*, No. 118290.
(38) Wanyonyi, F. S.; Fidelis, T. T.; Mutua, G. K.; Orata, F.; Pembere, A. M. S. Role of Pore Chemistry and Topology in the Heavy Metal Sorption by Zeolites: From Molecular Simulation to

Machine Learning. *Comput. Mater. Sci.* **2021**, *195* (April), No. 110519.
(39) Asif, K.; Lock, S. S. M.; Taqvi, S. A. A.; Jusoh, N.; Yiin, C. L.; Chin, B. L. F. A Molecular Simulation Study on Amine-Functionalized Silica/Polysulfone Mixed Matrix Membrane for Mixed Gas Separation. *Chemosphere* **2023**, *311* (P1), No. 136936.
(40) Huang, B.; Zhao, R.; Xu, H.; Deng, J.; Li, W.; Wang, J.; Yang, H.; Zhang, L. Adsorption of Methylene Blue on Bituminous Coal: Adsorption Mechanism and Molecular Simulation. *ACS Omega* **2019**, *4* (9), 14032−14039.
(41) Lock, S. S. M.; Lau, K. K.; Shariff, A. M.; Yeong, Y. F.; Bustam, M. A. Computational Insights on the Role of Film Thickness on the Physical Properties of Ultrathin Polysulfone Membranes. *RSC Adv.* **2017**, *7* (70), 44376−44393.
(42) Farrell, J.; Chaudhary, B. K. Understanding Arsenate Reaction Kinetics with Ferric Hydroxides. *Environ. Sci. Technol.* **2013**, *47* (15), 8342−8347.
(43) Asif, K.; Lock, S. S. M.; Taqvi, S. A. A.; Jusoh, N.; Yiin, C. L.; Chin, B. L. F.; Loy, A. C. M. A Molecular Simulation Study of Silica/Polysulfone Mixed Matrix Membrane for Mixed Gas Separation. *Polymers* **2021**, *13* (13), No. 2199.
(44) Yee, C. Y.; Lim, L. G.; Lock, S. S. M.; Jusoh, N.; Yiin, C. L.; Chin, B. L. F.; Chan, Y. H.; Loy, A. C. M.; Mubashir, M. A Systematic Review of the Molecular Simulation of Hybrid Membranes for Performance Enhancements and Contaminant Removals. *Chemosphere* **2022**, *307* (P3), No. 135844.
(45) Zhang, X.; Shi, X.; Deng, M.; Wang, Y.; Ning, P.; Tang, L.; Ning, Z. Stability Study of the As(V)-Fe(III) Oxyhydroxide Coprecipitate over a Broad PH Range: Characteristics and Mechanism. *Sci. Total Environ.* **2022**, *806*, No. 150794.
(46) Yadav, A.; Dindorkar, S. S.; Ramisetti, S. B.; Sinha, N. Simultaneous Adsorption of Methylene Blue and Arsenic on Graphene, Boron Nitride and Boron Carbon Nitride Nanosheets: Insights from Molecular Simulations. *J. Water Process Eng.* **2022**, *46*, No. 102653.
(47) Guo, Q. G.; Li, Y.; Zheng, L.-W.; Wei, X.-Y.; Xu, Y.; Shen, Y.-W.; Zhang, K.-G.; Yuan, C.-G. Facile Fabrication of Fe/Zr Binary MOFs for Arsenic Removal in Water: High Capacity, Fast Kinetics and Good Reusability. *J. Environ. Sci.* **2023**, *128* (2023), 213−223.
(48) Suhaimi, N. H.; Jusoh, N.; Rashidi, S. S.; Ch'ng, C. W. M.; Sambudi, N. S. Ethylene Recovery via Pebax-Based Composite Membrane: Numerical Optimization. *Sustainability* **2023**, *15* (3), 1856.
(49) Heng, G. C.; Isa, M. H.; Lock, S. S. M.; Ng, C. A. Process Optimization of Waste Activated Sludge in Anaerobic Digestion and Biogas Production by Electrochemical Pre-Treatment Using Ruthenium Oxide Coated Titanium Electrodes. *Sustainability* **2021**, *13* (9), 4874.
(50) Jiang, N.; Erdős, M.; Moultos, O. A.; Shang, R.; Vlugt, T. J. H.; Heijman, S. G. J.; Rietveld, L. C. The Adsorption Mechanisms of Organic Micropollutants on High-Silica Zeolites Causing S-Shaped Adsorption Isotherms: An Experimental and Monte Carlo Simulation Study. *Chem. Eng. J.* **2020**, *389* (November 2019), No. 123968.
(51) Xu, W.; Wang, J.; Wang, L.; Sheng, G.; Liu, J.; Yu, H.; Huang, X. J. Enhanced Arsenic Removal from Water by Hierarchically Porous CeO2-ZrO2 Nanospheres: Role of Surface- and Structure-Dependent Properties. *J. Hazard. Mater.* **2013**, *260*, 498−507.
(52) Lim, D. T.; Tuyen, T. N.; Nhiem, D. N.; Duc, D. H.; Chuc, P. N.; Bac, N. Q.; Tung, D. X.; Pham, N. N.; Ha, L. T. V.; Tu, N. T. T.; Nguyen, V. T.; Khieu, D. Q. Fluoride and Arsenite Removal by Adsorption on La2O3-CeO2/Laterite. *J. Nanomater.* **2021**, *2021*, No. 9991050.
(53) Cui, H.; Li, Q.; Gao, S.; Shang, J. K. Strong Adsorption of Arsenic Species by Amorphous Zirconium Oxide Nanoparticles. *J. Ind. Eng. Chem.* **2012**, *18* (4), 1418−1427.
(54) Guan, X.; Du, J.; Meng, X.; Sun, Y.; Sun, B.; Hu, Q. Application of Titanium Dioxide in Arsenic Removal from Water: A Review. *J. Hazard. Mater.* **2012**, *215*−*216*, 1−16.
(55) Rahmanifar, B.; Moradi Dehaghi, S. Removal of Organochlorine Pesticides by Chitosan Loaded with Silver Oxide Nanoparticles from Water. *Clean Technol. Environ. Policy* **2014**, *16* (8), 1781−1786.
(56) Iakovleva, E.; Maydannik, P.; Ivanova, T. V.; Sillanpää, M.; Tang, W. Z.; Mäkilä, E.; Salonen, J.; Gubal, A.; Ganeev, A. A.; Kamwilaisak, K.; Wang, S. Modified and Unmodified Low-Cost Iron-Containing Solid Wastes as Adsorbents for Efficient Removal of As(III) and As(V) from Mine Water. *J. Cleaner Prod.* **2016**, *133*, 1095−1104.
(57) Gupta, A. D.; Rene, E. R.; Giri, B. S.; Pandey, A.; Singh, H. Adsorptive and Photocatalytic Properties of Metal Oxides towards Arsenic Remediation from Water: A Review. *J. Environ. Chem. Eng.* **2021**, *9* (6), No. 106376.
(58) Kumar, K. Y.; Raj, T. N. V.; Archana, S.; Prasad, S. B. B.; Olivera, S.; Muralidhara, H. B. SnO2 Nanoparticles as Effective Adsorbents for the Removal of Cadmium and Lead from Aqueous Solution: Adsorption Mechanism and Kinetic Studies. *J. Water Process Eng.* **2016**, *13*, 44−52.
(59) Wang, Y.; Liu, Y.; Guo, T.; Liu, H.; Li, J.; Wang, S.; Li, X.; Wang, X.; Jia, Y. Lanthanum Hydroxide: A Highly Efficient and Selective Adsorbent for Arsenate Removal from Aqueous Solution. *Environ. Sci. Pollut. Res.* **2020**, *27* (34), 42868−42880.
(60) Lin, T. F.; Wu, J. K. Adsorption of Arsenite and Arsenate within Activated Alumina Grains: Equilibrium and Kinetics. *Water Res.* **2001**, *35* (8), 2049−2057.
(61) Lock, S. S. M.; Lau, K. K.; Shariff, A. M.; Yeong, Y. F.; Bustam, M. A.; Jusoh, N.; Ahmad, F. An Atomistic Simulation towards Elucidation of Operating Temperature Effect in CO2 Swelling of Polysulfone Polymeric Membranes. *J. Nat. Gas Sci. Eng.* **2018**, *57*, 135−154.
(62) Friesecke, G.; Theil, F. Molecular Geometry Optimization, Models. *Encyclopedia of Applied and Computational Mathematics* **2015**, 951.
(63) Zhang, X.; Zhao, Y.; Zhang, Z.; Wang, S. Investigation of the Interaction between Xanthate and Kaolinite Based on Experiments, Molecular Dynamics Simulation, and Density Functional Theory. *J. Mol. Liq.* **2021**, *336*, No. 116298.
(64) Rappe, A. K.; Casewit, C. J.; Colwell, K. S.; Goddard, W. A., III.; W, M. S. UFF, a Full Periodic Table Force Field for Molecular Mechanics and Molecular Dynamics Simulations. *J. Am. Chem. Soc.* **1992**, *114* (25), 10024−10035.
(65) Akkermans, R. L. C.; Spenley, N. A.; Robertson, S. H. Monte Carlo Methods in Materials Studio. *Mol. Simul.* **2013**, *39* (14−15), 1153−1164.
(66) Zawierta, M.; Platek, B.; Falat, T.; FFelba, J. In *Coarse Grained Molecular Dynamics Study of Heat Transfer in Thermal Interface Materials*, Proceedings of the 36th International Spring Seminar on Electronics Technology, Alba Iulia, Romania, 2013; pp 259−262.
(67) Bahamon, D.; Khalil, M.; Belabbes, A.; Alwahedi, Y.; Vega, L. F.; Polychronopoulou, K. A DFT Study of the Adsorption Energy and Electronic Interactions of the SO_2 molecule on a CoP Hydrotreating Catalyst. *RSC Adv.* **2021**, *11* (5), 2947−2957.
(68) Ghose, S. K.; Waychunas, G. A.; Trainor, T. P.; Eng, P. J. Hydrated Goethite (α-FeOOH) (1 0 0) Interface Structure: Ordered Water and Surface Functional Groups. *Geochim. Cosmochim. Acta* **2010**, *74* (7), 1943−1953.
(69) Hounfodji, J. W.; Kanhounnon, W. G.; Kpotin, G.; Atohoun, G. S.; Lainé, J.; Foucaud, Y.; Badawi, M. Molecular Insights on the Adsorption of Some Pharmaceutical Residues from Wastewater on Kaolinite Surfaces. *Chem. Eng. J.* **2021**, *407* (September 2020), No. 127176.
(70) Liu, X.; Tu, Y.; Liu, S.; Liu, K.; Zhang, L.; Li, G.; Xu, Z. Adsorption of Ammonia Nitrogen and Phenol onto the Lignite Surface: An Experimental and Molecular Dynamics Simulation Study. *J. Hazard. Mater.* **2021**, *416* (April), No. 125966.
(71) Yang, H.; Lu, R.; Downs, R. T.; Costin, G. Goethite, α-FeO(OH), from Single-Crystal Data. *Acta Crystallogr. Sect. E* **2006**, *62* (12), i250−i252.

https://doi.org/10.1021/acsomega.3c07014
ACS Omega 2023, 8, 48130−48144

(72) Wu, M.; Zhao, S.; Tang, M.; Jing, R.; Shao, Y.; Liu, X.; Dong, Y.; Li, M.; Liao, Q.; Lv, G.; Zhang, Q.; Meng, Z.; Liu, A. Adsorption of Sulfamethoxazole and Tetracycline on Montmorillonite in Single and Binary Systems. *Colloids Surf., A* **2019**, *575* (March), 264−270.
(73) Li, L.; He, M.; Feng, Y.; Wei, H.; You, X.; Yu, H.; Wang, Q.; Wang, J. X. Adsorption of Xanthate from Aqueous Solution by Multilayer Graphene Oxide: An Experimental and Molecular Dynamics Simulation Study. *Adv. Compos. Hybrid Mater.* **2021**, *4* (3), 725−732.
(74) Moradi, H.; Azizpour, H.; Mohammadi, M. Study of Adsorption of Propane and Propylene on CHA Zeolite in Different Si/Al Ratios Using Molecular Dynamics Simulation. *Powder Technol.* **2023**, *419*, No. 118329.
(75) Sheldon, C.; Paier, J.; Sauer, J. Adsorption of CH4on the Pt(111) Surface: Random Phase Approximation Compared to Density Functional Theory. *J. Chem. Phys.* **2021**, *155* (17), No. 174702.
(76) Kokalj, A.; Dlouhy, M. Dissociative Adsorption of Azoles on Cu(111) Promoted by Chemisorbed O and OH. *Corros. Sci.* **2022**, *209* (May), No. 110680.
(77) Ullah, F.; Bashiri, R.; Muti Mohamed, N.; Zaleska-Medynska, A.; Kait, C. F.; Ghani, U.; Shahid, M. U.; Saheed, M. S. M. Exploring Graphene Quantum Dots@TiO2 Rutile (0 1 1) Interface for Visible-Driven Hydrogen Production in Photoelectrochemical Cell: Density Functional Theory and Experimental Study. *Appl. Surf. Sci.* **2022**, *576* (PB), No. 151871.
(78) Ba Mohammed, B.; Yamni, K.; Tijani, N.; Alrashdi, A. A.; Zouihri, H.; Dehmani, Y.; Chung, I. M.; Kim, S. H.; Lgaz, H. Adsorptive Removal of Phenol Using Faujasite-Type Y Zeolite: Adsorption Isotherms, Kinetics and Grand Canonical Monte Carlo Simulation Studies. *J. Mol. Liq.* **2019**, *296*, No. 111997.
(79) Abdelhameed, R. M.; Taha, M.; Abdel-Gawad, H.; Mahdy, F.; Hegazi, B. Zeolitic Imidazolate Frameworks: Experimental and Molecular Simulation Studies for Efficient Capture of Pesticides from Wastewater. *J. Environ. Chem. Eng.* **2019**, *7* (6), No. 103499.
(80) Bayantong, A. R. B.; Shih, Y.-J.; Ong, D. C.; Abarca, R. R. M.; Dong, C.-Di.; de Luna, M. D. G. Adsorptive Removal of Dye in Wastewater by Metal Ferrite-Enabled Graphene Oxide Nanocomposites. *Chemosphere* **2021**, *274*, No. 129518.
(81) Bigdeli, A.; Khorasheh, F.; Tourani, S.; Khoshgard, A.; Bidaroni, H. H. Molecular Simulation Study of the Adsorption and Diffusion Properties of Terephthalic Acid in Various Metal Organic Frameworks. *J. Inorg. Organomet. Polym. Mater.* **2020**, *30* (5), 1643−1652.
(82) Düren, T.; Bae, Y. S.; Snurr, R. Q. Using Molecular Simulation to Characterise Metal−Organic Frameworks for Adsorption Applications. *Chem. Soc. Rev.* **2009**, *38* (5), 1237−1247.
(83) Zhang, J.; Lu, X.; Shi, C.; Yan, B.; Gong, L.; Chen, J.; Xiang, L.; Xu, H.; Liu, Q.; Zeng, H. Unraveling the Molecular Interaction Mechanism between Graphene Oxide and Aromatic Organic Compounds with Implications on Wastewater Treatment. *Chem. Eng. J.* **2019**, *358* (October 2018), 842−849.
(84) Zhang, Q.; Han, Y.; Wu, L. Influence of Electrostatic Field on the Adsorption of Phenol on Single-Walled Carbon Nanotubes: A Study by Molecular Dynamics Simulation. *Chem. Eng. J.* **2019**, *363* (January), 278−284.
(85) Pathan, S.; Bose, S. Arsenic Removal Using "Green" Renewable Feedstock-Based Hydrogels: Current and Future Perspectives. *ACS Omega* **2018**, *3* (5), 5910−5917.
(86) Nicomel, N. R.; Leus, K.; Folens, K.; Van Der Voort, P.; Du Laing, G. Technologies for Arsenic Removal from Water: Current Status and Future Perspectives. In *Int. J. Environ. Res. Public Health*, MDPI December 22, 2015 DOI: 10.3390/ijerph13010062.
(87) Takagi, S.; Adachi, F.; Miyano, K.; Koizumi, Y.; Tanaka, H.; Watanabe, I.; Tanabe, S.; Kannan, K. Fate of Perfluorooctanesulfonate and Perfluorooctanoate in Drinking Water Treatment Processes. *Water Res.* **2011**, *45* (13), 3925−3932.
(88) Hong, S.; Xian-chun, T.; Nan-xiang, W.; Hong-bin, C. Leakage of Soluble Microbial Products from Biological Activated Carbon Filtration in Drinking Water Treatment Plants and Its Influence on Health Risks. *Chemosphere* **2018**, *202*, 626−636.
(89) Irunde, R.; Ijumulana, J.; Ligate, F.; Maity, J. P.; Ahmad, A.; Mtamba, J.; Mtalo, F.; Bhattacharya, P. Arsenic in Africa: Potential Sources, Spatial Variability, and the State of the Art for Arsenic Removal Using Locally Available Materials. In *Groundwater for Sustainable Development*; Elsevier B.V., August 1, 2022 DOI: 10.1016/j.gsd.2022.100746.
(90) Condit, W.; Chen, A.; Wang, L.; Wang, A. *Arsenic Removal from Drinking Water by Iron Removal and Adsorptive Media: U.S. EPA Demonstration Project at Stewart, MN, Final Performance Evaluation Report*; 2009.
(91) Jusoh, N.; Yeong, Y. F.; Lau, K. K.; M Shariff, A. Transport Properties of Mixed Matrix Membranes Encompassing Zeolitic Imidazolate Framework 8 (ZIF-8) Nanofiller and 6FDA-Durene Polymer: Optimization of Process Variables for the Separation of CO2from CH4. *J. Cleaner Prod.* **2017**, *149*, 80−95.
(92) Solangi, Z. A.; Bhatti, I.; Qureshi, K. A Combined CFD-Response Surface Methodology Approach for Simulation and Optimization of Arsenic Removal in a Fixed Bed Adsorption Column. *Processes* **2022**, *10* (9), No. 1730.
(93) Waqar, A.; Bheel, N.; Almujibah, H. R.; Benjeddou, O.; Alwetaishi, M.; Ahmad, M.; Sabri, M. M. S. Effect of Coir Fibre Ash (CFA) on the Strengths, Modulus of Elasticity and Embodied Carbon of Concrete Using Response Surface Methodology (RSM) and Optimization. *Results Eng.* **2023**, *17* (March), No. 100883.
(94) Ali, A. M.; Kwaya, M. Y.; Mijinyawa, A.; Aminu, A. A.; Usman, Z. M. Molecular Dynamics and Energy Distribution of Methane Gas Adsorption in Shales. *J. Nat. Gas Geosci.* **2023**, *8* (1), 1−15.
(95) Caporale, A. G.; Punamiya, P.; Pigna, M.; Violante, A.; Sarkar, D. (2013). Effect of Particle Size of Drinking-Water Treatment Residuals on the Sorption of Arsenic in the Presence of Competing Ions. *J. Hazard. Mater.* **2013**, *260*, 644−651.
(96) Li, M.; Liu, J.; Xu, Y.; Qian, G. Phosphate Adsorption on Metal Oxides and Metal Hydroxides: A Comparative Review. *Environ. Rev.* **2016**, *24*, 319−332.
(97) Kumar, K. Y.; Raj, T. V.; Archana, S.; Prasad, S. B.; Olivera, S.; Muralidhara, H. B. (2016). SnO2 Nanoparticles as Effective Adsorbents for the Removal of Cadmium and Lead from Aqueous Solution: Adsorption Mechanism and Kinetic Studies. *J. Water Process Eng.* **2016**, *13*, 44−52.
(98) Yang, H.; Min, X.; Xu, S.; Wang, Y. Lanthanum(III)-Coated Ceramics as a Promising Material in Point-of-Use Water Treatment for Arsenite and Arsenate Removal. *ACS Sustainable Chem. Eng.* **2019**, *7* (10), 9220−9227.
(99) Luo, Q.; Li, G.; Chen, M.; Qin, F.; Li, H.; Qiang, Y. Effect Factor of Arsenite and Arsenate Removal by a Manufactured Material: Activated Carbon-Supported Nano-TiO2. *J. Chem.* **2020**, *2020*, No. 6724157.
(100) Zhang, W.; Singh, P.; Paling, E.; Delides, S. Arsenic Removal from Contaminated Water by Natural Iron Ores. *Miner. Eng.* **2004**, *17* (4), 517−524.
(101) Kyzas, G. Z.; Lazaridis, N. K.; Mitropoulos, A. C. Removal of Dyes from Aqueous Solutions with Untreated Coffee Residues as Potential Low-Cost Adsorbents: Equilibrium, Reuse and Thermodynamic Approach. *Chem. Eng. J.* **2012**, *189−190*, 148−159.
(102) Paredes-Laverde, M.; Salamanca, M.; Diaz-Corrales, J. D.; Flórez, E.; Silva-Agredo, J.; Torres-Palma, R. A. Understanding the Removal of an Anionic Dye in Textile Wastewaters by Adsorption on ZnCl2activated Carbons from Rice and Coffee Husk Wastes: A Combined Experimental and Theoretical Study. *J. Environ. Chem. Eng.* **2021**, *9* (4), No. 105685.
(103) Li, R.; Wang, J. J.; Zhou, B.; Awasthi, M. K.; Ali, A.; Zhang, Z.; Gaston, L. A.; Lahori, A. H.; Mahar, A. Enhancing Phosphate Adsorption by Mg/Al Layered Double Hydroxide Functionalized Biochar with Different Mg/Al Ratios. *Sci. Total Environ.* **2016**, *559*, 121−129.
(104) Tang, Q.; Shi, C.; Shi, W.; Huang, X.; Ye, Y.; Jiang, W.; Kang, J.; Liu, D.; Ren, Y.; Li, D. Preferable Phosphate Removal by Nano-

La(III) Hydroxides Modified Mesoporous Rice Husk Biochars: Role of the Host Pore Structure and Point of Zero Charge. *Sci. Total Environ.* **2019**, *662*, 511−520.
(105) Pillai, P.; Kakadiya, N.; Timaniya, Z.; Dharaskar, S.; Sillanpaa, M. Removal of Arsenic Using Iron Oxide Amended with Rice Husk Nanoparticles from Aqueous Solution. In *Materials Today: Proceedings*; Elsevier Ltd., 2019; Vol. *28*, pp 830−835 DOI: 10.1016/j.matpr.2019.12.307.
(106) More, H. Factors Affecting Adsorption. 2020. https://thefactfactor.com/facts/pure_science/chemistry/physical-chemistry/factors-affecting-adsorption/11184/.
(107) Wang, C.; Luo, H.; Zhang, Z.; Wu, Y.; Zhang, J. C. S.; Chen, S. Removal of As(III) and As(V) from Aqueous Solutions Using Nanoscale Zero Valent Iron-Reduced Graphite Oxide Modified Composites. *J. Hazard. Mater.* **2014**, *268*, 124−131, DOI: 10.1016/j.jhazmat.2014.01.009.
(108) Rathi, B. S.; Kumar, P. S. Application of adsorption process for effective removal of emerging contaminants from water and wastewater. *Environmental Pollution* **2021**, *280*, 116995.

https://doi.org/10.1021/acsomega.3c07014
ACS Omega 2023, 8, 48130−48144